The Calculation of the Axion Mass from Lattice QCD

Z. Fodor, J. N. Guenther

published in

NIC Symposium 2018
K. Binder, M. Müller, A. Trautmann (Editors)

Forschungszentrum Jülich GmbH,
John von Neumann Institute for Computing (NIC),
Schriften des Forschungszentrums Jülich, NIC Series, Vol. 49,
ISBN 978-3-95806-285-6, pp. 187.
http://hdl.handle.net/2128/17544

The Calculation of the Axion Mass from Lattice QCD

Zoltan Fodor[1,2,3] **and Jana N. Guenther**[4]

[1] Department of Physics, University of Wuppertal, 42119 Wuppertal, Germany
E-mail: fodor@theorie.physik.uni-wuppertal.de

[2] Jülich Supercomputing Centre, Forschungszentrum Jülich, 52425 Jülich, Germany

[3] Institute for Thoretical Physics, Eötvös University, 1117 Budapest, Hungary

[4] Institute for Theoretical Physics, Regensburg University, 93053 Regensburg, Germany

Based on S. Borsanyi *et al.*, "Calculation of the axion mass based on high-temperature lattice quantum chromodynamics", Nature **539** (2016) no.7627, 69 we present the results of a large scale computation for the equation of state of the strong and electroweak interaction as well as the topological susceptibility. Both are calculated over a large range in temperature. Together these two quantities allow for an estimation of the axion mass, a promising dark matter candidate.

1 Introduction

The behaviour of the early universe can be described by the equation of state of the strong and electroweak interaction. The theory of the strong interaction, Quantum Chromo Dynamics (QCD)[1], is symmetric under time reversal, which leads to a fine tuning problem. A solution to this problem is the introduction of a new particle: the axion[2,3]. It appears as the Goldstone boson of an additional, spontaneously broken $U(1)$ symmetry, the so called Peccei-Quinn-symmetry. This is very attractive because the axion is also a promising dark matter candidate. As our standard model of particle physics describes only about five percent of the matter in our universe, identifying components of dark matter is an important research subject (reviews can be found in Ref. 4, 5). For an experimental search for theoretically proposed particles a profound knowledge of characteristics of these particles is important. Under the assumption that axions are the dominant constituent of dark matter, their mass can be predicted from the equation of state and the temperature dependence of the topological susceptibility of QCD.

The strong coupling of QCD makes it unsuited for investigations with perturbation theory, the common approach for solving quantum field theories. To obtain quantitative results from first principle QCD one uses lattice calculations, where the continuous space time is discretised on a four dimensional lattice[6]. This approach is computationally very demanding. Here we report on our calculations for the equation of state and the topological susceptibility, a specially challenging quantity, that leads to an estimation of the axion mass $m_A = 50$ - 1500 μeV in an post-inflation scenario. A large part of the computation necessary for this determination was carried out on the JUQUEEN supercomputer of the Jülich Supercomputing Centre.

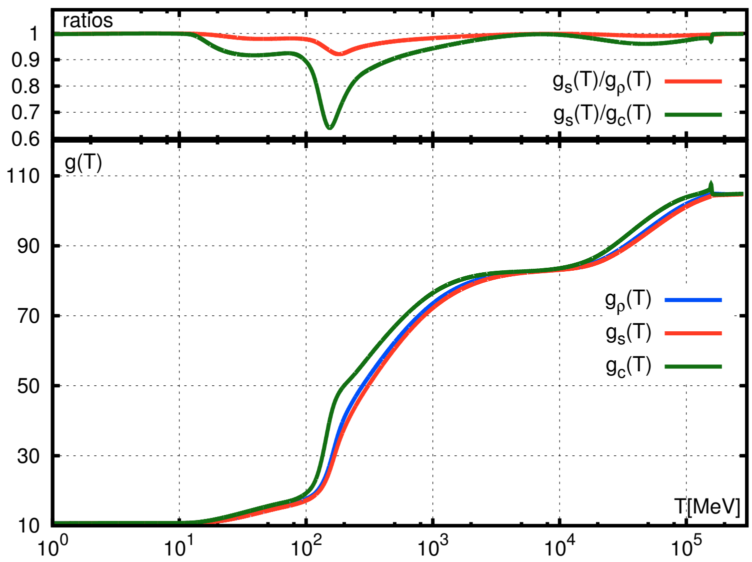

Figure 1. The effective degrees of freedom g_ρ for the energy density ($\rho = g_\rho \frac{\pi^2}{30} T^4$), g_s for the entropy density $s = g_s \frac{2\pi^2}{45} T^3$, and g_c for the heat capacity ($c = g_c \frac{2\pi^2}{15} T^3$).

2 The Equation of State

The details of our analysis and the lattice setup can be found in Ref. 7. For a complete description of the thermal evolution of the early universe an equation of state over a very large temperature range is needed. Therefore we have to supplement our lattice calculations for QCD with the rest of the Standard Model particles (leptons, heavy quarks, weak gauge bosons and the Higgs boson) as well as results that describe the electroweak transition. The final result that is shown in the Figs. 1 and 2 covers four orders of magnitude between MeV and hundreds of GeV. The line width in Fig. 1 represents the uncertainties. In Fig. 2 one can see that the transitions between the 2+1 lattice results up to 250 MeV, the 2+1+1 lattice results up to 500 MeV and the perturbative calculations for even higher temperatures are very smooth. The full result is tabulated in Ref. 7.

This equation of state can now be used to calculate the Hubble expansion rate of the universe $H(T)$ similar as it is done in Ref. 8. As described in Sec. 4 this can be used to calculate the axion mass.

3 The Topological Susceptibility

A problem one encounters while computing the topological susceptibility on the lattice, is that for the topological susceptibility staggered quarks have very large cutoff effects. This can be reduced by a technique called *Eigenvalue reweighting* introduced in Sec. 3.1. Another difficulty is that it takes very long to sample different topological sectors. This can be circumvented by the *fixed sector integral method* described in Sec. 3.2.

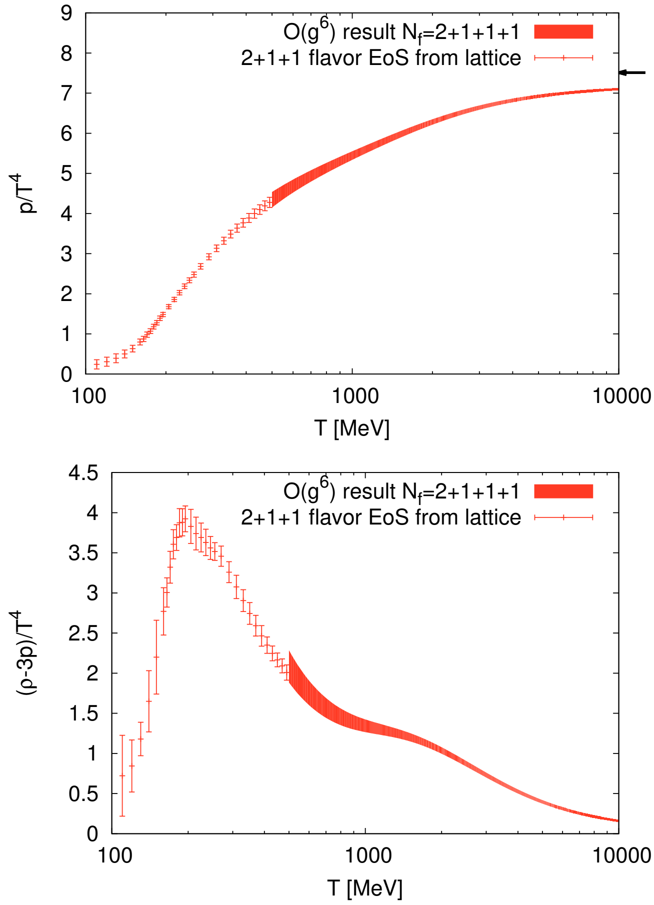

Figure 2. The QCD pressure and the trace anomaly in the 2+1+1+1 theory.

3.1 Eigenvalue Reweighting

In Fig. 3 it can be seen, that the continuum behaviour of the topological susceptibility with staggered fermions is problematic. For the brute force approach, that is shown by the green points, it is not possible to make a linear continuum extrapolation. To obtain the correct continuum limit very fine lattices are needed. For Fig. 3 lattices up to $N_t = 20$ were used.

The strong cutoff effects of the staggered fermions are related to the fact, that on the lattice the would be zero Eigenmodes are not exactly zero in the staggered operator. The zero modes split up and contribute two modes slightly above and two modes lightly below zero for the staggered operator.

A zero mode in the quark determinant contributes a factor $2m_f$ to the weight of configuration in the topological susceptibility for every dynamical flavour. Since for quark masses close to the physical ones m_f is very small, configurations with zero modes, corresponding to higher topological sectors, are strongly suppressed. However when the stag-

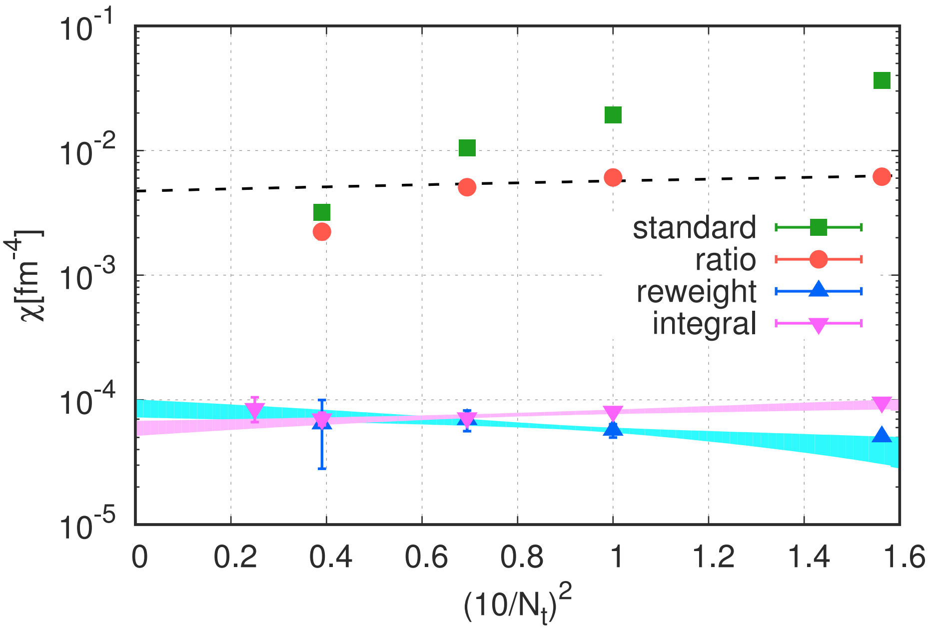

Figure 3. Lattice spacing dependence of the topological susceptibility obtained from four different methods described in the text: standard, ratio, reweighting and integral.

gered operator is used, instead of a factor $2m_f$ one gets a factor $2m_f + \mathrm{i}\lambda_0$ where λ_0 is the would-be Eigenmode of the staggered operator. Therefore the suppression is much milder, increasing the influence of higher topological sectors. This leads to large cutoff effects and a slow convergence to the continuum. The idea of the Eigenvalue reweighting technique is to bring the weight closer to the continuum weight for each configuration. Fig. 3 illustrates the success of this method. The standard approach, shown in green, does not allow for a linear extrapolation. Another approach the so called *ratio method*[9], which results are displayed in red, allows for an extrapolation from the $N_t = 8, 10$ and 12 lattices as hinted by the dashed line. However the result of the $N_t = 16$ lattice proves that this extrapolation is strongly misleading. Any extrapolation from this two methods would be very steep. On the other hand the continuum extrapolation through the blue points, obtained from the reweighting method, is relatively flat. It also agrees with the results from the *integral Method*, plotted in pink, that is constructed for high temperatures and described in the next section.

3.2 The Fixed Sector Integral Method

The dilute instanton gas approximation (DIGA)[10,11] can be used to estimate the topological susceptibility $\chi(T)$ at high temperatures. It predicts a power law behaviour of the form T^{-b} with $b = 8.16$. In Ref. 12 the exponent of this power law has been calculated in quenched

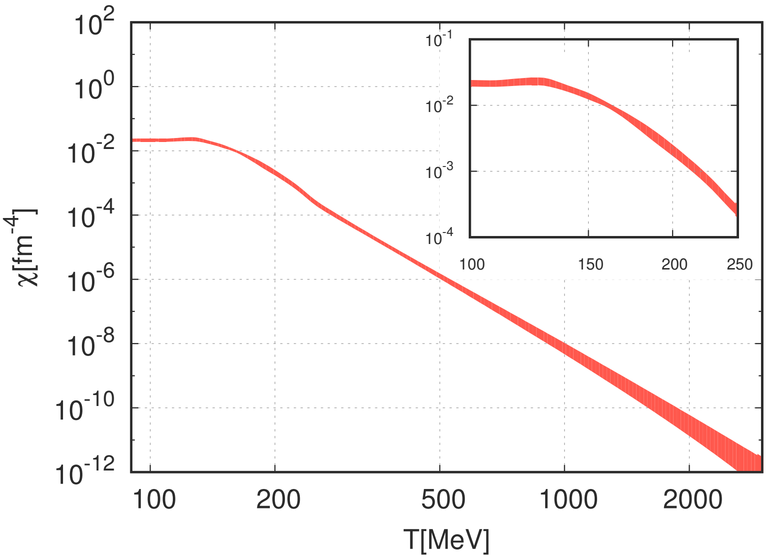

Figure 4. The final result in the continuum limit of the topological susceptibility $\chi(T)$. The enhancement shows the behaviour around the transition temperature. The width of the line represents the combined statistical and systematic errors.

lattice simulations to be about $b = 7$. As it can be seen in Fig. 4, this means that the topological susceptibility decreases rapidly with increasing temperature and agrees well with the results from the DIGA. Thus for hight temperatures the weight of the $Q = 0$ sectors increases. This makes it harder to measure $\chi(T)$, for which the ratio between the different sectors is needed. Also for smaller lattice spacings the simulation stays longer in one topological sector as shown in Ref. 13. Both points lead to the need for very long streams at hight temperatures and small lattice spacing. There are some methods that increase the tunnelling between different topological sectors[14–16]. However here we are using a different method that was developed simultaneously in Ref. 17 (for quenched QCD) and Ref. 7 (also for fermions). The idea of this method is to do simulations in fixed topological sectors and than calculate the weight for the different topological sectors. If the temperature is high enough the only relevant sectors for appropriate volumes are $Q = 1$ and $Q = 0$. Several numerical test, as well as another trick to further decreases the computation time are discussed in Ref. 7. Overall this new method reduces the CPU cost tremendously by changing the scaling with the temperature from T^8 as in conventional techniques to almost T^0.

4 Calculation of the Axion Mass

After calculating the topological susceptibility $\chi(T)$ and the Hubble expansion rate $H(T)$, this two results can be used to calculate the amount of axionic dark matter and the axion mass. As it can be seen in Fig. 4, $\chi(T)$ is decreasing rapidly with the temperature. Since

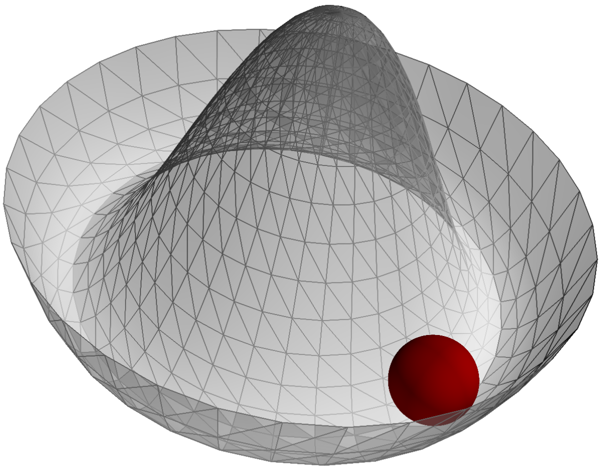

Figure 5. The illustration of the tilted Mexican hat like Peccei-Quinn potential. The rolling down axion field is shown by the read ball.

the axion mass m_A is proportional to $\chi(T)^{1/2}$ it is so small at hight temperatures, or early in the expansion of the universe, that it is frozen by the Hubble friction. The increasing topological susceptibility tilts the Mexican hat like Peccei-Quinn potential. The tilt is not yet felt by the axion, which therefore remains effectively massless. While the topological susceptibility and the axion mass increases with time, the Hubble expansion decreases. The oscillation time $T_{\rm osc}$ is defined as $3H(T_{\rm osc}) = m_A(T_{\rm osc})$. At this time the axion mass is of the same order as the Hubble constant and the axion field starts to roll down the Peccei-Quinn potential, as illustrated in Fig. 5. It oscillates around the minimum of the tilted potential, which leads to the production of axions. This production mechanism is called misalignment. A detailed description can be found in Ref. 18.

The value of the misalignment angle θ depends on whether one assumes a post- or pre-inflationary scenario. In a post-inflationary scenario θ can initially vary between $-\pi$ and π. Therefore we have to average over the different angles, resulting in an average angle of $\theta_0 = 2.155$ (for details on the averaging procedure see the Supplementary Information of Ref. 7). This angle is depicted in red in Fig. 6. On the other hand in a pre-inflationary scenario all angles but one θ_0 are inflated away. The relation between θ_0 and the axion mass is shown in Fig. 6 by the blue line. The uncertainty vanishes within the line width. One can see a slight bend of the blue line at $m_A \sim 10^{-5}$ μeV. It corresponds to an oscillation temperature at the QCD transition[19,20].

An other production mechanism one should take into account is the decay of cosmological strings. They appear during the $U(1)$ symmetry breaking and produce dark matter axions during their decay. In a pre-inflationary scenario they are not relevant as they are inflated away, but in a post-inflationary scenario their role is important. Since this axion production mechanism is less well understood one has to make some assumptions to reach a final result.

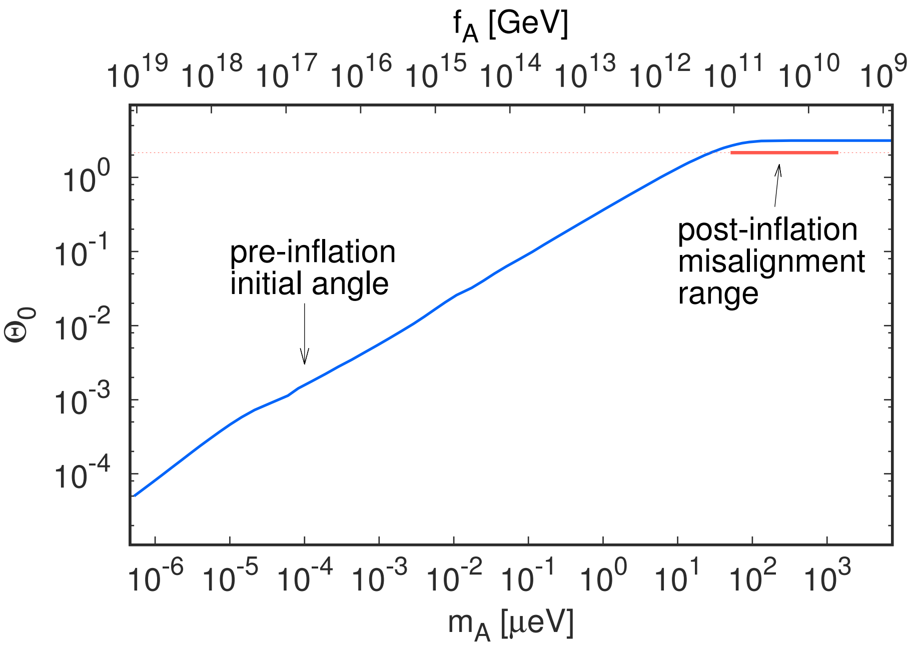

Figure 6. The relation between the axion mass and the initial angle θ_0.

From the post-inflationary scenario we get a strict lower bound on the axion mass of $m_A = 28(2)$ μeV. If one assumes that between 1% and 50% of the dark matter are axions from the misalignment mechanism this leads to the mass range between $m_A = 50$ μeV and 1500 μeV that is depicted in red in Fig. 6.

Acknowledgements

We thank Szabolcs Borsanyi, Karl-Heinz Kampert, Sandor D. Katz, Taichi Kawanai, Tamas G. Kovacs, Simon W. Mages, Attila Pasztor, Ferenc Pittler, Javier Redondo, Andreas Ringwald and Kalman K. Szabo for the fruitful collaboration. For the useful discussions we thank M. Dierigl, M. Giordano, S. Krieg, D. Nogradi and B. Toth. This project was funded by the DFG grant SFB/TR55, and by OTKA under grant OTKA-K-113034. The work of J. R. is supported by the Ramon y Cajal Fellowship 2012-10597 and FPA2015- 65745-P (MINECO/FEDER). The computations were performed on JUQUEEN at Forschungszentrum Jülich, on SuperMUC at Leibniz Supercomputing Centre in München, on Hazel Hen at the High Performance Computing Center in Stuttgart, on QPACE in Wuppertal and on GPU clusters in Wuppertal and Budapest.

References

1. H. Fritzsch, M. Gell-Mann, and H. Leutwyler, *Advantages of the Color Octet Gluon Picture*, Phys. Lett., **47B**, 365–368, 1973.
2. S. Weinberg, *A New Light Boson?*, Phys. Rev. Lett., **40**, 223–226, 1978.
3. F. Wilczek, *Problem of Strong p and t Invariance in the Presence of Instantons*, Phys. Rev. Lett., **40**, 279–282, 1978.
4. G. Bertone, D. Hooper, and J. Silk, *Particle dark matter: Evidence, candidates and constraints*, Phys. Rept., **405**, 279–390, 2005.
5. J. L. Feng, *Dark Matter Candidates from Particle Physics and Methods of Detection*, Ann. Rev. Astron. Astrophys., **48**, 495–545, 2010.
6. K. G. Wilson, *Confinement of Quarks*, Phys. Rev., **D10**, 2445–2459, 1974.
7. S. Borsanyi et al., *Calculation of the axion mass based on high-temperature lattice quantum chromodynamics*, Nature, **539**, no. 7627, 69–71, 2016.
8. K. A. Olive et al., *Review of Particle Physics*, Chin. Phys., **C38**, 090001, 2014.
9. C. Bonati, M. D'Elia, M. Mariti, G. Martinelli, M. Mesiti, F. Negro, F. Sanfilippo, and G. Villadoro, *Axion phenomenology and θ-dependence from $N_f = 2 + 1$ lattice QCD*, JHEP, **03**, 155, 2016.
10. G. 't Hooft, *Computation of the Quantum Effects Due to a Four-Dimensional Pseudoparticle*, Phys. Rev., **D14**, 3432–3450, 1976, [Erratum: Phys. Rev., **D18**, 2199, 1978].
11. C. G. Callan Jr., R. F. Dashen, and D. J. Gross, *Toward a Theory of the Strong Interactions*, Phys. Rev., **D17**, 2717, 1978.
12. S. Borsanyi, M. Dierigl, Z. Fodor, S. D. Katz, S. W. Mages, D. Nogradi, J. Redondo, A. Ringwald, and K. K. Szabo, *Axion cosmology, lattice QCD and the dilute instanton gas*, Phys. Lett., **B752**, 175–181, 2016.
13. S. Schaefer, R. Sommer, and F. Virotta, *Critical slowing down and error analysis in lattice QCD simulations*, Nucl. Phys., **B845**, 93–119, 2011.
14. A. Laio, G. Martinelli, and F. Sanfilippo, *Metadynamics surfing on topology barriers: the CP^{N1} case*, JHEP, **07**, 089, 2016.
15. M. Luscher and S. Schaefer, *Lattice QCD without topology barriers*, JHEP, **07**, 036, 2011.
16. S. Mages, B. C. Toth, S. Borsanyi, Z. Fodor, S. D. Katz, and K. K. Szabo, *Lattice QCD on nonorientable manifolds*, Phys. Rev., **D95**, 094512, 2017.
17. J. Frison, R. Kitano, H. Matsufuru, S. Mori, and N. Yamada, *Topological susceptibility at high temperature on the lattice*, JHEP, **09**, 021, 2016.
18. O. Wantz and E. P. S. Shellard, *Axion Cosmology Revisited*, Phys. Rev., **D82**, 123508, 2010.
19. Y. Aoki, S. Borsanyi, S. Durr, Z. Fodor, S. D. Katz, S. Krieg, and K. K. Szabo, *The QCD transition temperature: results with physical masses in the continuum limit II.*, JHEP, **06**, 088, 2009.
20. S. Borsanyi, Z. Fodor, C. Hoelbling, S. D. Katz, S. Krieg, C. Ratti, and K. K. Szabo, *Is there still any T_c mystery in lattice QCD? Results with physical masses in the continuum limit III*, JHEP, **09**, 073, 2010.